The effect of NMR-invisible susceptibility inclusions on phase maps.

S. J. Wharton[1], and R. Bowtell[1]
[1]Sir Peter Mansfield Magnetic Resonance Centre, University of Nottingham, Nottingham, United Kingdom

Introduction: Phase images generated using GE sequences at high field show exquisite anatomical contrast (1). This results from small changes of the NMR frequency that are linked to variation of the local magnetic susceptibility across tissues. Previous analysis of this phase contrast has generally focused on the effect of the average magnetic susceptibility in a particular compartment (1, 2), but it was recently pointed out that in the case where a significant contribution to the average susceptibility comes from non-spherical inclusions that do not generate an NMR signal, the average NMR frequency offset is not simply proportional to the average susceptibility (3). The analysis presented by He and Yablonskiy (3) focuses largely on the case of cylindrical inclusions, which are representative of iron-rich oligodendrocytes in white matter, and they introduced the idea of replacing the conventional sphere of Lorentz (4) with a Lorentzian ellipsoid in order to account for the shape of the inclusions. Their analysis showed in particular that the average NMR frequency offset in a long cylinder containing long, cylindrical, NMR-invisible inclusions is independent of the susceptibility of these inclusions. Here, we extend the previous work by developing a simple expression based on the use of the conventional sphere of Lorentz, which allows the average NMR frequency offset to be calculated for compartments containing NMR invisible inclusions of varying shape and concentration.

Theory: We consider the situation shown schematically in Fig. 1, where the sample consists of many identical, ellipsoidal inclusions of magnetic susceptibility, χ_2, embedded in a matrix of susceptibility, χ_1, confined to the shape, S, outside which the susceptibility is zero. We calculate the average NMR frequency offset as the sum of the effect of a shape, S, of uniform susceptibility, χ_1, plus that of a distribution of inclusions of susceptibility, χ_2-χ_1. The average frequency offset produced by the uniform shape, S, is given by $\Delta f_1 = f_0\chi_1\left(\frac{1}{3} - D_{zs}\right)$, where $f_0 = \gamma B_0$, D_{zs} is the z-demagnetizing factor of the overall sample shape (5) and the factor of 1/3 is the contribution of the sphere of Lorentz. To evaluate the effect of the inclusions on the average frequency offset, we assume that they are present in low concentration, and are randomly distributed, and first consider the field due to a single inclusion, in the two regions shown in Fig. 1. Inside the ellipsoid (Region A), the offset is given by $\Delta f_A = f_0(\chi_2 - \chi_1)\left(\frac{1}{3} - D_{ze}\right)$ where D_{ze} is the z-demagnetizing factor of the ellipsoid. Using the fact that the integral of the frequency offset due to magnetic sources inside a spherical volume must be zero (6), the average frequency in region B is given by $\Delta f_B = -\Delta f_A(V_A/V_B)$, where V_A and V_B represent the volumes of the two regions. We must finally add in a contribution to the average frequency offset, given by $\Delta f_C = f_0 v(\chi_2 - \chi_1)\left(\frac{1}{3} - D_{zs}\right)$, which represents the effect of the other inclusions which are randomly distributed inside the sample (v is the fraction of the sample volume taken up by the inclusions).

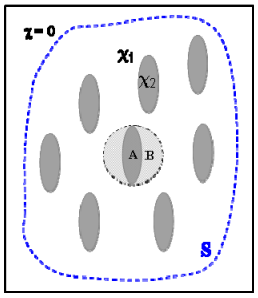

***Figure 1** –Schematic showing ellipsoidal inclusions.*

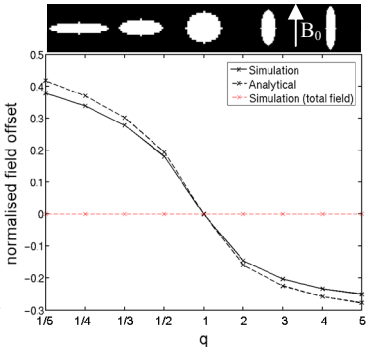

***Figure 2** –Plot of analytical and simulated $\Delta f/(v(\chi_2 - \chi_1)$ values against q of ellipsoids.*

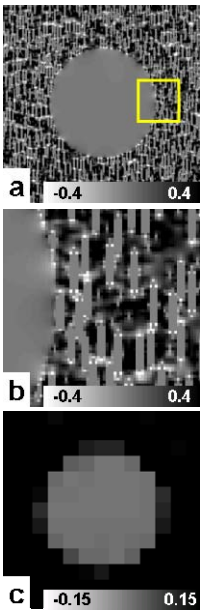

***Figure 3** –(a) Simulated frequency ,map for needle-like inclusions surrounding sphere of the same average volume susceptibility. (b) Magnified view of boxed region in (a); (c) Coarse resolution phase map with zero inclusion signal.*

Combining the contributions in the situation where the inclusions do generate an NMR signal, the effects of Δf_A and Δf_B cancel, yielding an average frequency offset given by Eq. [1] which, as would be expected, is equivalent to that occurring in a sample of shape, S, with a uniform susceptibility, χ_{av}, equal to the volume average of the susceptibility over the sample. More interestingly, when the ellipsoids generate no signal, the Δf_A contribution is lost and the resulting average frequency offset, which is now described by Eq. [2], cannot be represented using the volume average susceptibility alone.

$$\frac{\Delta f}{f_0} = \chi_1\left(\frac{1}{3} - D_{zs}\right) + v\left[\Delta f_A + \Delta f_B V_B/V_A + (\chi_2 - \chi_1)\left(\frac{1}{3} - D_{zs}\right)\right] = ((1-v)\chi_1 + v\chi_2)\left(\frac{1}{3} - D_{zs}\right) \quad [1]$$

$$\frac{\Delta f}{f_0} = \chi_{av}\left(\frac{1}{3} - D_{zs}\right) - v(\chi_2 - \chi_1)\left(\frac{1}{3} - D_{ze}\right) = \chi_1\left(\frac{1}{3} - D_{zs}\right) + v(\chi_2 - \chi_1)(D_{ze} - D_{zs}) \quad [2]$$

Inspection of Eq. [2] shows that the change in the relative frequency offset due to loss of signal from the ellipsoidal inclusions, depends on their volume fraction and shape, and on the difference of their susceptibility from that of the surrounding matrix. The extra term takes a value of zero, as would be expected, for spherical inclusions for which, D_{ze}=1/3, and can be either negative or positive when $\chi_2 > \chi_1$ depending whether the inclusion has a demagnetizing factor that is lower (prolate) or higher (oblate) than that of a sphere. It is also evident from this expression that the inclusions will have no effect on Δf when their shape is the same as that of the larger sample, such that D_{ze}=D_{zs}; this is in agreement with the findings of He and Yablonskiy (2), who described this effect for cylindrical inclusions inside a long cylinder.

Method: To test the theory, we simulated the frequency perturbations produced by random arrangements of identical ellipsoids contained inside a spherical matrix, using a Fourier-based method (3) that takes account of the effect of the sphere of Lorentz. Simulations were carried out for different ellipsoids of revolution, which were characterised by their aspect ratio $q = a_1/a_2$ (see shapes at the top of Fig. 2) where a_1 is the ellipsoid's length along the symmetry axis and a_2 is the size along the orthogonal directions, for an inclusion volume fraction of 1%. The frequency shift averaged over the whole sample and also excluding the inside of the ellipsoids was calculated in each case and the results compared with the theory described above, using standard expressions for the z-demagnetizing factor of an ellipsoid (5). In addition, we simulated the phase maps that would be produced for small Δf, when a spherical region of uniform susceptibility is surrounded by material of equal volume average susceptibility, but in which there are needle-like, NMR-invisible, paramagnetic inclusions aligned with the field ($D_{ze} \sim 0.1$).

Results and Discussion: Figure 2 shows that the average frequency offset in the simulated data is zero, as expected from Eq. [1] for a spherical sample (D_{zs} = 1/3), when the signal from inside the ellipsoids is included (blue line). When the signal from inside the ellipsoids is lost, the simulations (black continuous line) and theory (black dotted line) show that there is a non-zero frequency offset which varies from negative to positive as q increases from zero. The agreement between theory and simulation is good (small deviations result from the finite spatial resolution of the simulations). Figure 3c shows that two regions with identical volume average susceptibility, but different compartmentalisation of material, can have different intensities in phase images, and that the image shows a sharp boundary between regions. The effect shown in Fig. 3 might explain sharply defined phase changes observed in MS lesions (7) where demyelination may be accompanied by redistribution of iron. The simple analysis outlined here can be used to predict the expected phase contrast in other situations where there is a significant contribution to the average susceptibility from NMR invisible inclusions.

References: **[1]** Duyn et al. 2007. PNAS 104:11796 **[2]** He and Yablonskiy 2009. PNAS 106:13558 **[3]** Schäfer et al. Neuroimage. 2009. 48:126 **[4]** Durrant et al. 2003 Concepts in MR 18A: 72 **[5]** Ulrich et al 2003 JMR 164: 115 **[6]** Jackson, Classical Electrodynamics, Wiley 1998. **[7]** Haacke et al. 2009. JMRI. 29:537-544.